Design and Control of a Bi-directional *CLLC* Resonant Converter For Low voltage Energy Storage Systems

Ajeet K. Dhakar[1*], *Member, IEEE*, Abhinav Soni[2*], *Student*, Hari Om Bansal[3], *Senior Member IEEE*
[12]*Central Electronics Engineering Research Institute-CSIR, Rajasthan-333031*
[3]*Birla Institute of Technology & Science, Rajasthan-333031*
India

***Abstract*— This paper presents the design of a bi-directional *CLLC* converter with an Integrated transformer for energy storage systems (ESS) applications (48 V batteries). As the distributed energy generation and storage is gaining momentum it Is required to have ESS that can regulated the power bi-directionally, presently the ESS are bulky in size, to enhance the power density and converter efficiency, an integrated transformer is introduced and simulated using 3D Finite Element Analysis (FEA). Essentially, a simple PI-based voltage/current control loop Is implemented on a 32-bit microcontroller (TMS320F28379D). Also, synchronous rectification (SR) Is implemented by controlling the turn-on and turn-off delays on rectifier sides, respectively. The design and control of the CLLC converter are verified through the experimental results. A 300 kHz, 700 W prototype Is built with the peak conversion efficiency of 96.6% while charging and 96.4% while discharging**

Keywords—CLLC converter, Energy Storage System (ESS), Finite Element Analysis (FEA), battery charging mode (BCM), and discharging (DM)

I. INTRODUCTION

DC Distribution systems are gaining momentum to be the future's power system. As with the increasing demands, conventional energy sources are consumed at an exponential rate and are on the verge of extinction. The wide adoption of renewable energy sources would help to reduce the carbon footprint in the environment. Distributed generation can wave off some burden on the utility grid by storing surplus power during peak-off hours and supply the same during peak-on hours. The bi-directional converters are becoming an everlasting key component in the Distributed Generation (DG), due to its ability to condition power from a high-voltage (HV) distribution bus (Intermediate 400V DC link, or Variable 400-800V DC link, DC Electronic Load) to low-voltage (LV) distribution bus, to provide clean and stable output power and enable high reliability, effectiveness, and control of power systems. The DC distribution systems require a bi-directional AC-DC converter, which consists of a non-isolated AC-DC converter (power factor correction) and an isolated DC-DC converter (IBDC), authors in [18] developed a bi-directional AC-DC converter for DC distribution systems. Fig. 1 shows a DC-DC ESS unit converting power from an HV bus to LV batteries and vice versa.

The *CLLC* and DAB are two widely adopted topologies for DC-DC bi-directional power conversion [3][4]; the soft-switching ability is challenging to achieve in DAB converter thus, requires complex control to modulate the phase shifts

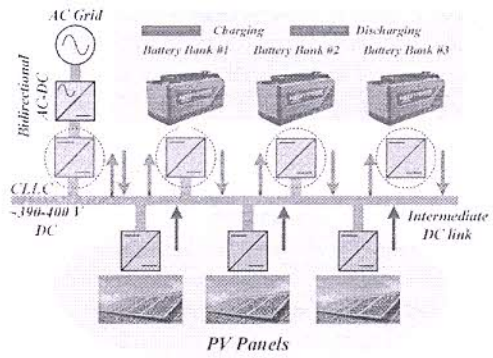

Fig. 1 *CLLC* resonant converter in a low voltage (LV) bus based Energy Storage System (ESS)

like in [16][17] the author proposes a Dual-Phase Shift (DPS) and Triple Phase Shift (TPS) modulation control. In contrast, the *CLLC* resonant converter can achieve soft-switching for full load range, while using a very simple and easy to implement control scheme of frequency modulation (FM) [2][3][7]. The implementation of bi-directional converters in [4-6][8][9] accounts for mostly (HV) outputs and no LV outputs; In the Indian scenario, the LV batteries are used for hybrid electric vehicle (HEVs), electric vehicle EVs and ESSs. In this regard, a bi-directional *CLLC* resonant converter is proposed to transfer power from an HV DC bus to LV batteries. The challenges in HV to LV power conversion is to deal with high output current in LV side which can cause severe conduction and termination loss; authors in [12][19] discusses a SR methodology; the losses due to body diode conduction can be mitigated if a synchronous rectification is used for LV sides in CM mode, respectively. A schematic of the full-bridge *CLLC* converter is shown in Fig. 2

Section II discusses the theoretical analysis of the *CLLC* converter, the FHA derived model of the *CLLC* converter,

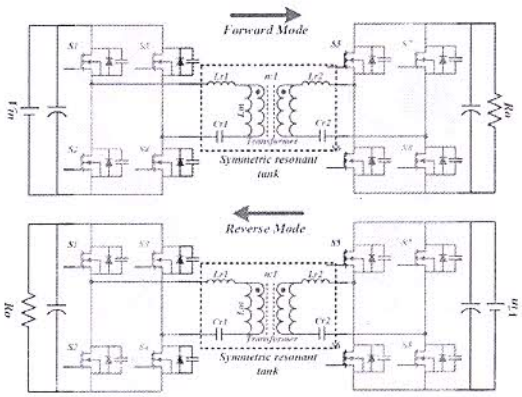

Fig. 2 Topology of *CLLC* resonant converter in charging (BCM) and discharging (DM) modes

978-1-7281-6916-3/20/$31.00 ©2020 IEEE

CM/DM mode analysis, and deduction of gain curves. Section III presents the design methodology of the *CLLC* converter for battery charging applications. Section IV presents a closed-loop control employing voltage loop control and current loop control of the *CLLC* resonant converter for charging (BCM) and discharging modes (DM). Section V presents a

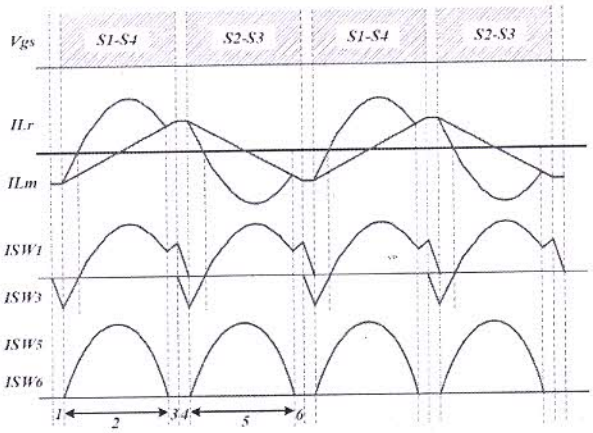

Fig. 3 Operating modes of the CLLC resonant converter at below resonance

synchronous rectification methodology for a full-bridge *CLLC* resonant converter. Ultimately, section VI concludes the design with experimental hardware results.

II. THEORETICAL ANALYSIS

Fig. 3 illustrates the waveforms for steady stage operation of the *CLLC* resonant converter operating below the resonant frequency.

A. Operation of CLLC Resonant Converter

Mode I represent a deadtime duration, during which all switches are turned off and no power is transferred to the secondary rectifying stage. The primary resonant current I_{Lr}, charges output capacitance of S_3, S_4 and discharges the output capacitance of S_1, S_2. After this process, the primary current passes through the anti-parallel diode of S_1 and S_2 which makes the switches operate under ZVS.

In II mode S_1, S_2 turns on and power is transferred through the transformer. The I_{Lr} reverses its direction to positive according to S_1, S_2 because the input source forces the current to positive direction through S_1, S_2, the output voltage from the secondary is impressed on the magnetizing inductance L_m, then the magnetizing current I_{Lm} , builds up linearly. Therefore, L_m does not participate in the resonance of the primary stage.

In mode III I_{Lr} equals magnetizing current, at this instant, the power transfer is stopped. Therefore, the secondary current I_s becomes zero, and the output capacitor is not charged by the output current. The I_{Lm} will keep rising till S_1, S_2 are turned off. During this mode, the L_m is no longer clamped by the output voltage. Thus, L_r, C_r and L_m participates in resonance together, and the resonant frequency of this mode is slightly different from other modes.

Mode IV is also a deadtime duration with the switch pair S_3, S_4. The operation is much similar to the mode I; however, the sequence of charging and discharging switches pair is different. The I_{Lr} discharges the output capacitances of S_3, S_4 and charges the output capacitances of S_1, S_2; and S_4, S_5 can turn on with ZVS.

In mode V S_3, S_4 turn on and starts transferring power to the secondary side. During this mode, the I_{Lr} changes direction due to the impressed voltage but now in the opposite

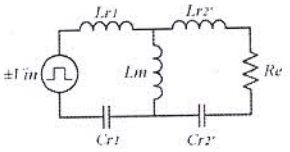

Fig. 5 FHA equivalent circuit of *CLLC* converter in DM operation

direction to that in mode II.

After the execution of Mode 5, the resonance and power transfer stops. With no power, the I_s becomes zero and the anti-parallel didoes of output rectifier are softly commutated. A similar operation occurs in the reverse mode, only load, and supply voltage changes.

B. Gain Analysis of CLLC Resonant Converter

i. Equivalent Circuit while charging (BCM)

The equivalent circuit of the *CLLC* converter in the forward mode is shown in Fig. 4. Assuming that 'n' is the transformer's turns ratio. Using the FHA, equivalent load resistance R_e can be expressed as follows [2][4][5][9].

$$R_e = \frac{8n^2}{\pi^2} R_o \tag{1}$$

Where, R_o is the load resistance in the forward mode. All the equivalent resonant parameters referred to the primary side are as follows.

$$L'_{r2} = n^2 L_{r2}, C'_{r2} = \frac{C_{r2}}{n^2}, \tag{2}$$

The normalized frequency, quality factor, and the resonant frequency is defined as (3)

$$\omega = \frac{\omega_s}{\omega_r}, Q_f = \frac{\sqrt{\frac{L_{r1}}{C_{r1}}}}{R_e}, \omega_r = \frac{1}{\sqrt{L_{r1} C_{r1}}} \tag{3}$$

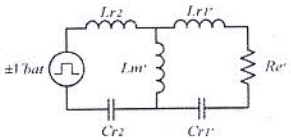

Fig. 4 FHA equivalent circuit of *CLLC* converter in BCM operation

ii. Equivalent Circuit while discharging (DM)

The Equivalent circuit of the *CLLC* converter in reverse mode is shown in Fig. 5, similar to (1) the equivalent load resistance (R_e') can be calculated using FHA [2][5] and is shown in (4)

$$R_e' = \frac{8}{n^2 \pi^2} R'_o \tag{4}$$

Where, R'_o is the load resistance in reverse mode. Similarly, all the resonant parameters referred to the secondary side are as follows.

$$L'_{r1} = \frac{L_{r1}}{n^2}, C_{r1} = n^2 C_{r1}, \omega_r = \frac{1}{\sqrt{L_{r2} C_{r2}}}$$

$$Q_r = \frac{\sqrt{\frac{L_{r2}}{C_{r2}}}}{R_e'}, \; L'_m = \frac{L_m}{n^2} \tag{5}$$

iii. Transfer function of CLLC converter

The general transfer function $H(s)$ can be derived by analyzing Fig. 4 and is expressed in (6)

$$H(s) = \frac{nVout}{Vin} = \frac{R_e(R_2//sL_m)}{R_2(sL_{r1}+\frac{1}{sC_{r1}}+R_2sL_m)} = \frac{Vin}{\left(\frac{1}{sC_{r1}}+sL_{r1}\right)+\left(n^2sL_{r2}+\frac{n^2}{sC_{r2}}+\frac{8n^2}{\pi^2}R_o\right)[1+\frac{1}{sL_m}(\frac{1}{sC_{r1}}+sL_{r1})]} \quad (6)$$

Where,

$$R_2 = R_e + sn^2L_{r2} + \frac{n^2}{sC_{r2}} \quad (7)$$

The gain function of *CLLC* converter in the forward mode is derived in [5], which could be expressed as (8)

$$|H(s)|_f = \frac{nV_{out}}{V_{in}} = \frac{1}{\sqrt{((\frac{1}{h}-\frac{1}{h\omega^2}+1)^2+[\frac{1}{\omega}(\frac{m}{h}+\frac{1}{hg}+\frac{1}{g}+1)Q_f-\omega(\frac{m}{h}+m+1)Q_f-\frac{Q_f}{hg\omega^3}]^2)}} \quad (8)$$

Where,

$$h = \frac{L_m}{L_{r1}}, m = \frac{n^2L_{r2}}{L_{r1}}, g = \frac{C_{r2}}{n^2C_{r1}}$$

Similarly, the gain function for reverse mode can be expressed as in (9)

$$|H(s)|_r = \frac{1}{\sqrt{((\frac{1}{p}-\frac{1}{p\omega^2}+1)^2+[\frac{1}{\omega}(\frac{r}{p}+\frac{1}{pq}+\frac{1}{q}+1)Q_r-\omega(\frac{r}{p}+r+1)Q_r-\frac{Q_r}{pq\omega^3}]^2)}} \quad (9)$$

Where,

$$p = \frac{L_m}{n^2L_{r2}}, r = \frac{L_{r1}}{n^2L_{r2}}, q = \frac{n^2C_{r1}}{C_{r2}}$$

iv. Primary side zero voltage switching (ZVS) consideration

ZVS is achieved whenever the converter is operating in the inductive region or the slope of gain curves is negative. As mentioned in [2], to achieve ZVS on the primary side of the converter, the magnetizing current must be sufficient to discharge the output capacitances of the primary side MOSFETs (in this case GaN MOSFETs) within deadtime. Thus, the L_m should be limited to a maximum value [2], given by (10)

$$L_m \leq \frac{T_{dead}}{16C_{oss}f_{smax}} \quad (10)$$

Where, T_{dead} is the dead time, C_{oss} is the MOSFET junction capacitance, and f_{smax} is the maximum switching frequency.

III. Design Methodology

A. Considerations of Design Parameters

In this paper, the converter is designed with 700 W of output power rating. The input voltage range is chosen as 360-400 V DC and the output voltage range is 45-54 V DC. The resonant frequency F_r is selected 350 kHz for charging (BCM) and 300 kHz for discharging (DM) modes considering the trade-offs between EMI, power density, and efficiency. Reducing the resonant frequency can help in the reduction of core and copper losses in the transformer but, may cause severe EMI issues [14]. The resonant converters have advantages of operating at a wide input/output voltage range; the converter aims at charging an ESS battery pack of voltage range 42-54 V (13 Cell Li-Ion Pack). The turns ratio for the *CLLC* converter can be calculated as:

$$n = \frac{V_{in}}{V_{out}} = \frac{400}{50} = 8 \quad (11)$$

To maximize the converter's efficiency is it recommended to operate it at resonant frequency [10]; this reduces circulating power loss and minimizes the current distortion. It is desired to have monotonic gain curves to implement linear control (PI); if not, then the non-linear control scheme has to opt which increases the control complexity and is not preferred for this application. Smaller Q factor can provide monotonic gain curves, while a large Q factor facilitates narrow frequency range. The nominal output resistance in CM mode is 5Ω with 50 V output voltage and in DM mode is 330Ω with 400 V output voltage. Based on the turn ratio, the gain range is designed to be 0.9-1.08 in BCM mode and 0.92-1.1 in DM mode, respectively. This gain arrangement satisfies the wide output range requirement of the converter. The resonant elements can be calculated via equations (1-3) for charging mode and (4-5) for discharging modes; resonant capacitor and leakage inductance can be calculated as:

$$C_{r1} = \frac{1}{2\pi f_r Q_f R_e} \quad (12)$$

$$L_{r1} = \frac{1}{2\pi {f_r}^2 C_{r1}} \quad (13)$$

To reduce the size and weight of the converter, leakage inductance of the transformer is utilized as resonant inductors. Table. I enlist the designed parameters for the *CLLC* converter. Fig. 6 shows the MATLAB plotted gain curves for BCM and DM modes, respectively.

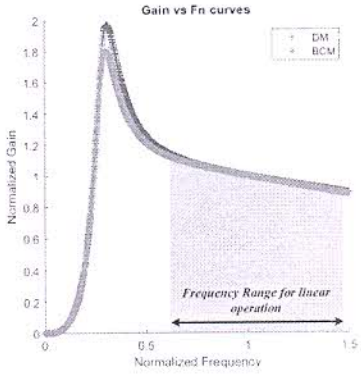

Fig. 6 Gain curves obtained via MATLAB plots for BCM and DM modes

TABLE I. KEY DESIGN PARAMETERS OF *CLLC* RESONANT CONVERTER

Parameters	Forward	Reverse
Resonant frequency F_r (kHz)	350	300
Gain range	0.9-1.08	0.98-1.06
Input Voltage Range (V)	340-380	40-60
Output voltage range (V)	40-60	360-400
Primary resonant capacitor C_{r1}	$11nF$	
Secondary resonant capacitor C_{r2}	$1\mu F$	
Primary resonant inductance L_{r1}	$17\mu H$	
Secondary resonant inductance L_{r2}	$260nH$	
Magnetizing inductance L_m	$120\mu H$	

B. Design of Integrated PlanarTransformer

To achieve high conversion efficiency, it is desired to mitigate core and winding losses; additionally, to reduce the weight and volume of the converter, an integrated transformer is adopted in this design. The windings are made of PCB stacks each for the primary and secondary sides. To utilize leakage inductances as resonant inductors, both primary and secondary windings are separated by a winding gap l_b; by varying this gap, the leakage inductance of both primary and secondary sides can be adjusted to the required value. An air gap is provided between core legs to avoid